Skeletal Radiol (2003) 32:375–387
DOI 10.1007/s00256-003-0618-0

REVIEW ARTICLE

Asif Saifuddin

Imaging tumours of the brachial plexus

Received: 31 July 2002
Revised: 19 September 2002
Accepted: 12 December 2002
Published online: 20 March 2003

A. Saifuddin (✉)
Department of Radiology,
The Royal National Orthopaedic Hospital NHS Trust,
Brockley Hill, Stanmore, HA7 4LP UK
e-mail: Asaifuddin@aol.com
Tel.: +44-208-9542300 ext 5443
Fax: +44-208-9540281

Abstract Tumours of the brachial plexus are rare lesions and may be classified as benign or malignant. Within each of these groups, they are further subdivided into those that are neurogenic in origin (schwannoma, neurofibroma and malignant peripheral nerve sheath tumour) and those that are non-neurogenic. Careful pre-operative diagnosis and staging is essential to the successful management of these lesions. Benign neurogenic tumours are well characterized with pre-operative MRI, appearing as well-defined, oval soft-tissue masses, which are typically isointense on T1-weighted images and show the "target sign" on T2-weighted images. Differentiation between schwannoma and neurofibroma can often be made by assessing the relationship of the lesion to the nerve of origin. Many benign non-neurogenic tumours, such as lipoma and fibromatosis, are also well characterized by MRI. This article reviews the imaging features of brachial plexus tumours, with particular emphasis on the value of MRI in differential diagnosis.

Keywords Brachial plexus · Neoplasm · Imaging · MRI

Introduction

The brachial plexus is not uncommonly involved by malignant tumours of the lung apex and breast, or as a result of radiotherapy. Less commonly, malignant bone tumours, such as osteosarcoma, arising from the cervical spine, clavicle or first rib may invade the plexus. However, primary lesions of the brachial plexus are rare. A review of the published literature between 1886 and 1987 revealed 147 patients with tumours involving the plexus, not including secondary extension from carcinomas of the lung or breast [1]. With regard to such tumours, important questions that need to be answered include whether or not the lesion is of neurogenic or non-neurogenic origin; if neurogenic, then whether it is benign or malignant; and if benign, whether it is a neurofibroma or schwannoma. Also, the local extent must be defined, particularly extension into the spinal canal.

Although the normal brachial plexus can be imaged with ultrasound (US) [2, 3] and the US appearances of benign nerve sheath tumours have been described [4, 5], tumours of the plexus are ideally imaged with magnetic resonance imaging (MRI). MRI is of proven value in imaging various pathological processes related to the brachial plexus [6, 7, 8, 9, 10, 11, 12, 13] and also in the characterization of neurogenic [14, 15, 16, 17, 18, 19, 20, 21, 22, 23] and non-neurogenic soft-tissue tumours [24, 25, 26]. This article reviews the relevant clinical and radiological features of primary tumours of the brachial plexus, with emphasis on the value of MRI in differential diagnosis and local staging.

Anatomical considerations

The anatomy of the brachial plexus is complex, comprising roots, trunks, divisions, cords and branches (Fig. 1) [12,13, 27]. The plexus arises from the ventral rami of the C5–T1 nerve roots, which lie between the anterior and middle scalene muscles, adjacent to the subclavian artery. At the lateral border of the scalene muscles, the rami combine to form upper, middle and lower trunks.

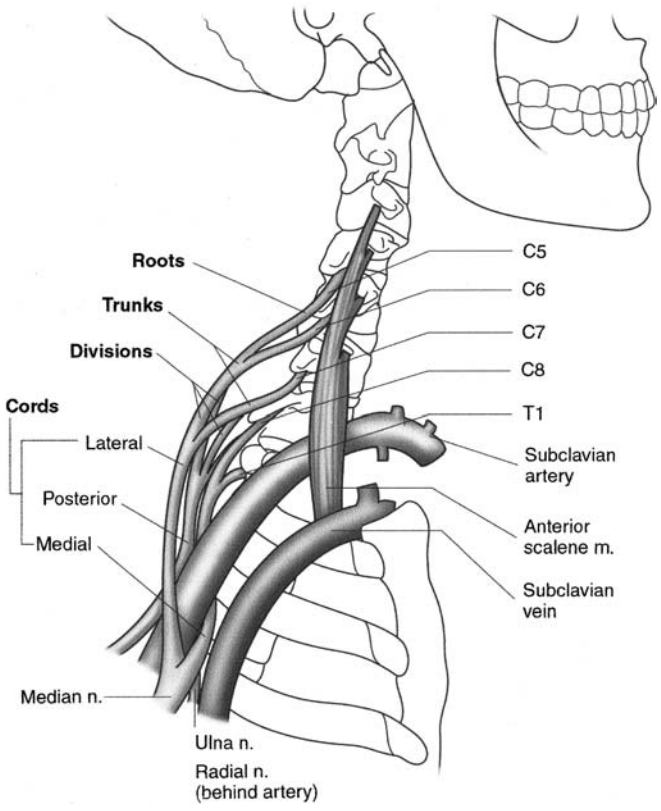

Fig. 1 The major anatomical relationships of the right brachial plexus

The roots and trunks comprise the *supraclavicular plexus*. The divisions are formed as the plexus passes posterior to the clavicle (the *retroclavicular plexus*) and they combine to produce the three cords at the lateral border of the first rib. The three cords are named according to their relationship to the subclavian artery, being lateral, posterior and medial. Just lateral to the pectoralis minor muscle, the cords divide into the terminal branches. The cords and branches comprise the *infraclavicular plexus*.

The brachial plexus is well imaged by MRI (Fig. 2). The roots of the plexus are best demonstrated on axial images as they exit the intervertebral foramina. The coronal plane also demonstrates various sections of the roots, trunks and cords. The three cords can be differentiated on sagittal images, where their relationship to the subclavian artery is optimally demonstrated [13].

There is no standard MRI technique for imaging the plexus. However, the combination of coronal T1-weighted spin echo (SE) and STIR sequences together with fat-suppressed axial dual echo T2-weighted fast spin echo (FSE) sequences will suffice in the majority of cases. A sagittal T1- or T2-weighted FSE sequence best demonstrates the relationship of a plexus tumour to the subclavian artery. Routine use of intravenous contrast enhancement is not required.

A basic knowledge of plexus anatomy is important since it allows the differentiation of tumours arising from the plexus from other anterior neck masses. Two factors must be considered. The first is the anatomical plane of the mass (Fig. 3). Tumours arising from the roots will lie between the anterior and middle scalene muscles. The second is the orientation of the mass. Primary neurogenic tumours are typically oval in shape and lie with their long axis parallel to the nerve of origin. Tumours arising from the upper roots will therefore run in an oblique direction from superomedial to inferolateral, whereas tumours from the lower roots will run in a horizontal direction. Tumours running in a vertical direction are unlikely to arise from the plexus (Fig. 4) [28].

Clinical and surgical considerations

Approximately 20% of peripheral nerve tumours arise in the brachial plexus [29]. Primary tumours of the brachial plexus may present as painless masses, or with varying combinations of paraesthesia, pain and neurological dysfunction. Examination findings include muscle weakness, wasting and a positive Tinel's sign [1, 29, 30, 31]. Cardinal clinical features of malignancy are pain at rest, which typically prevents the patient from sleeping and is resistant to opiates, progressive loss of neurological function [30] and rapid growth of a tumour in patients with neurofibromatosis type 1 (NF1).

Table 1 combines the results from two large series of primary neurogenic brachial plexus tumours collected over a period of 29 years [1, 32]. It is clear that the diagnosis of an individual lesion is related to the presence or absence of NF1 (von Recklinghausen's disease), which was present in 30% of cases. Neurofibromas account for over three-quarters of all lesions in the presence of NF1, and are commonly multiple and plexiform in nature [1]. Conversely, in the absence of NF1, over 50% of lesions will be solitary schwannomas. There is no significant difference in the incidence of malignant peripheral nerve sheath tumour (MPNST) between these two groups of patients.

The importance of pre-operative differentiation between schwannoma and neurofibroma lies in the functional outcome following excision, and thus in pre-operative counselling of the patient. Schwannoma is a well-encapsulated tumour that arises from the Schwann cell and displaces the nerve fascicles without infiltrating them. Therefore, surgical excision is usually possible without damaging the nerve. Conversely, plexiform neurofibromas infiltrate the nerve fascicles and complete resection of the tumour will consequently result in permanent nerve damage [13, 29]. Only solitary (as opposed to plexiform) neurofibromas can often be removed without nerve damage. With regard to MPNST, the major imaging challenge is the identification of occult, proximal in-

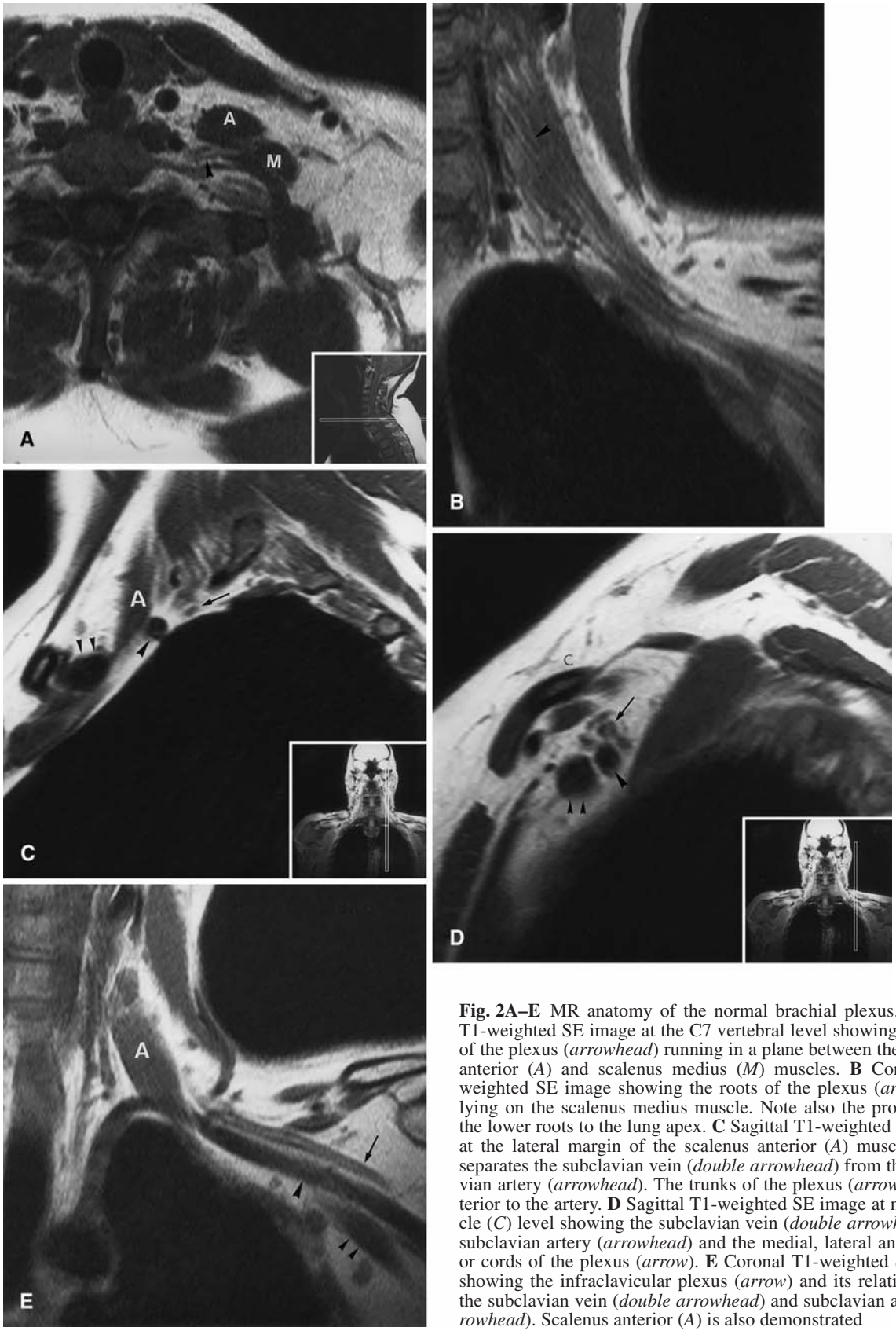

Fig. 2A–E MR anatomy of the normal brachial plexus. **A** Axial T1-weighted SE image at the C7 vertebral level showing the roots of the plexus (*arrowhead*) running in a plane between the scalenus anterior (*A*) and scalenus medius (*M*) muscles. **B** Coronal T1-weighted SE image showing the roots of the plexus (*arrowhead*) lying on the scalenus medius muscle. Note also the proximity of the lower roots to the lung apex. **C** Sagittal T1-weighted SE image at the lateral margin of the scalenus anterior (*A*) muscle, which separates the subclavian vein (*double arrowhead*) from the subclavian artery (*arrowhead*). The trunks of the plexus (*arrow*) lie posterior to the artery. **D** Sagittal T1-weighted SE image at mid-clavicle (*C*) level showing the subclavian vein (*double arrowhead*), the subclavian artery (*arrowhead*) and the medial, lateral and posterior cords of the plexus (*arrow*). **E** Coronal T1-weighted SE image showing the infraclavicular plexus (*arrow*) and its relationship to the subclavian vein (*double arrowhead*) and subclavian artery (*arrowhead*). Scalenus anterior (*A*) is also demonstrated

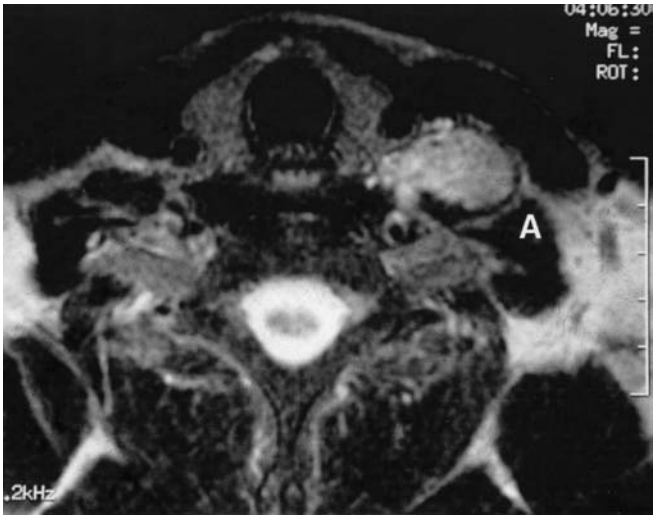

Fig. 3 Axial T2-weighted FSE image of a patient with a referral diagnosis of left brachial plexus tumour. However, the lesion is located in front of the scalenus anterior muscle (*A*) and therefore cannot be arising from the plexus. Histological diagnosis was synovial sarcoma

traneural spread. Intradural extension of these tumours renders the patient incurable by surgery alone. The relationship of any central lesion to the vertebral artery must also be determined. If a malignant lesion involves the vertebral artery, demonstration of a patent contralateral vertebral artery may be achieved by magnetic resonance angiography (MRA). However, if the vertebral artery has to be sacrificed, the circle of Willis will need to be investigated with conventional angiography and balloon occlusion of the ipsilateral vertebral artery, in order to determine the vascular supply to the posterior fossa from the contralateral vertebral artery (J. Allibone FRCS, Consultant Neurosurgeon, personal communication).

Table 2 combines the results from the same two series of primary non-neurogenic brachial plexus tumours [1, 32]. The commonest benign lesion was fibromatosis (extra-abdominal desmoid tumour), accounting for one-third of the tumours. Other reported tumours included lipoma (3 cases), myositis ossificans (3 cases), ganglioneuroma, haemangioma, lymphangioma, myoblastoma, localized hypertrophic neuropathy and branchial cleft cyst. A wide variety of malignant non-neurogenic tumours were seen, including metastases, osteosarcoma and Ewing sarcoma. Other reported benign non-neurogenic tumours include intraneural ganglion [33], elastofibroma [34] and fibrolipomatous hamartoma [35], whereas malignant non-neurogenic tumours include radiation-induced sarcomas [36, 37, 38], synovial sarcoma [39], lymphoma [40] and neuroblastoma [41].

Table 1 Combined results of two major published series of primary neurogenic brachial plexus tumours collected over a 29-year period and the relationship of neurogenic tumours to neurofibromatosis 1 (*NF1*) (*MPNST* malignant peripheral nerve sheath tumour) [1, 32]

Tumour	Number	Number with NF1
Neurofibroma	59 (49%)	29 (81%)
Schwannoma	44 (37%)	1 (3%)
MPNST	17 (14%)	6 (16%)
Total	120 (100%)	36 (100%)

Table 2 Combined results of two major published series of primary non-neurogenic brachial plexus tumours collected over a 29-year period [1, 32]

Tumour	Number
Benign non-neurogenic	21 (44%)
Malignant non-neurogenic	27 (56%)
Total	48 (100%)

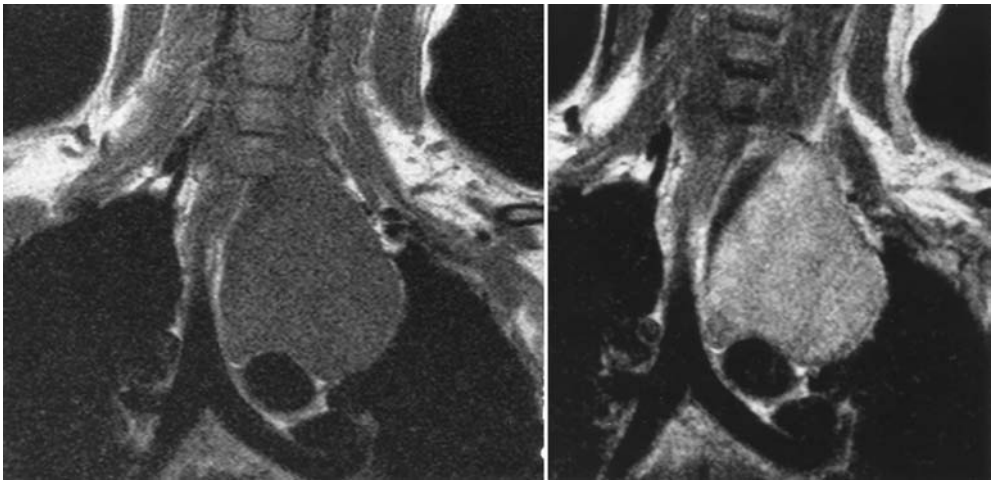

Fig. 4 Coronal T1-weighted SE image (*left*) and post-contrast T1-weighted SE image (*right*) of a patient with a superior mediastinal mass which is involving the lower roots of the left brachial plexus. The mass is orientated with its long axis in the vertical direction. At surgery, the lesion was found to be a schwannoma of the vagus nerve

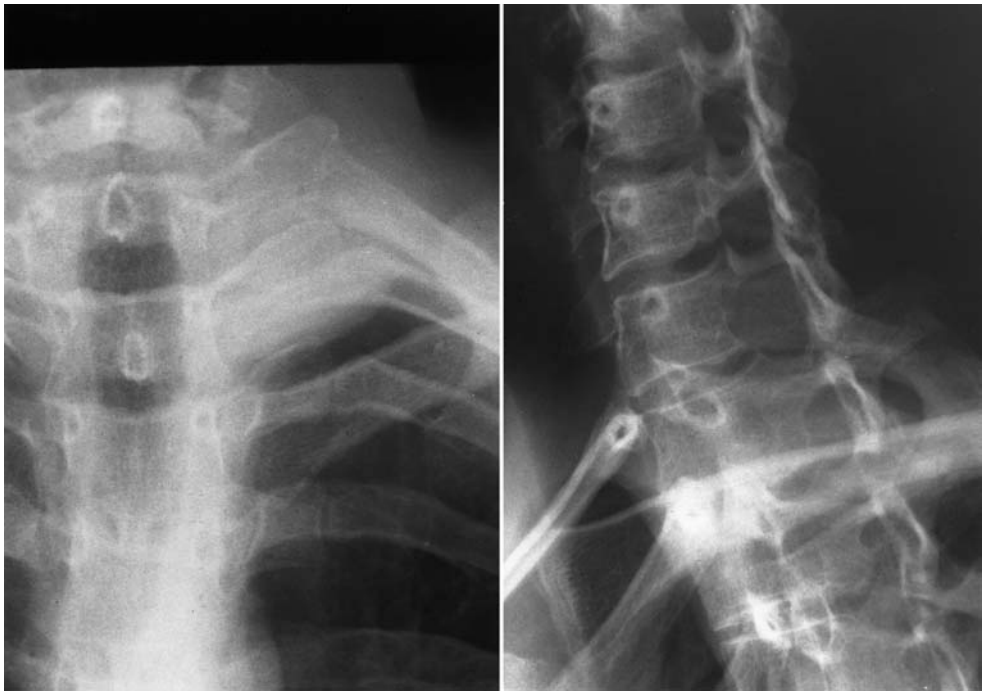

Fig. 5 Radiographic features of a brachial plexus tumour arising in relation to the C8 root. Expansion of the left C7/T1 neural foramen is identified on the oblique radiograph (*right*) while the extraspinal component produces a well-defined extrapleural mass in the left lung apex (*left*). The histological diagnosis was synovial sarcoma

Imaging findings

Neurofibroma and schwannoma

Radiography is usually normal unless the tumour has extended into the neural foramen, when it may cause well-defined bony erosion and foraminal enlargement. Tumours arising from the lower roots of the plexus can appear as an apical lung mass [42]. These features do not necessarily indicate a benign lesion or a primary neurogenic tumour (Fig. 5).

US demonstrates benign neurogenic tumours as well-defined, oval, homogeneous hypoechoic masses with posterior acoustic enhancement [4, 5, 23]. The absence of an echogenic central hilum helps differentiate these lesions from cervical lymph nodes [4]. However, an echogenic ring may be identified within a benign nerve sheath tumour [43].

Typical MR features of benign neurogenic tumours include a well-defined oval mass with the long axis in line with the nerve of origin and homogeneous intermediate signal intensity (SI) on T1-weighted sequences (Fig. 6). The tumours are hyperintense on T2-weighted images with inhomogeneous central low SI (the target sign) (Fig. 7) [19, 21] and strong enhancement following contrast administration (Fig. 8). The target sign is attributed to the distribution of Antoni A and B areas within the tumour. The peripheral hyperintense signal is due to myxoid tissue whereas the central hypointense area is related to a greater proportion of fibrocollagenous tissue [17, 19]. Less commonly, schwannomas and neurofibromas may be mildly hyperintense or hypointense to muscle on T1-weighted images and show non-uniform enhancement [17, 18, 19, 20, 22, 23]. The presence of the target sign does not differentiate neurofibroma from schwannoma [19]. However, schwannoma and neurofibroma can be distinguished by determining the relation-

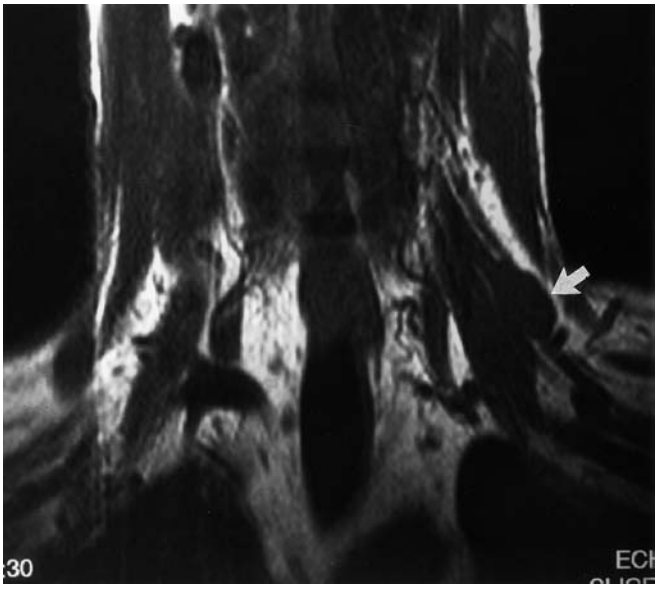

Fig. 6 Coronal T1-weighted SE image showing a small schwannoma (*arrow*) arising from a trunk of the left brachial plexus. The lesion is isointense to muscle and orientated in an oblique direction along the long axis of the nerve

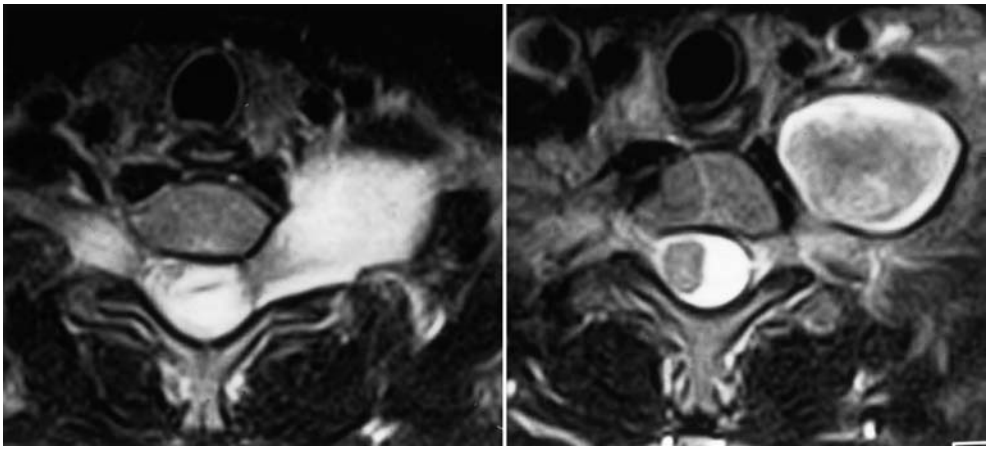

Fig. 7 Axial T2-weighted FSE image showing a large schwannoma arising from the left brachial plexus in a patient with neurofibromatosis type 1 (NF1). The lesion is hyperintense and displays the typical "target sign" that characterizes a benign nerve sheath tumour. Intraspinal extension with foraminal enlargement is also noted

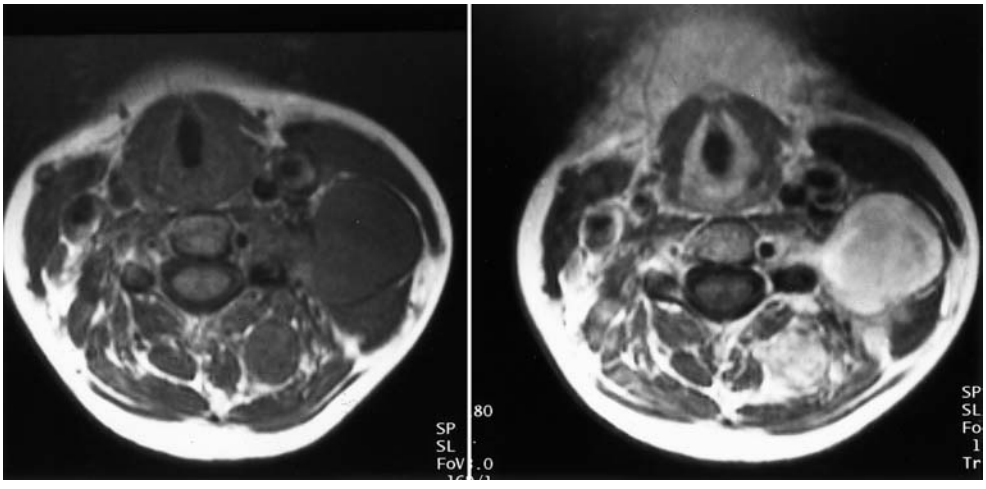

Fig. 8 Axial T1-weighted SE image of a patient with a schwannoma arising from the left brachial plexus. Pre-contrast image (*left*) shows the lesion to be homogeneous and isointense to muscle. Following gadolinium administration (*right*), the tumour shows inhomogeneous enhancement

ship of the tumour to the nerve of origin. In the case of schwannoma, the nerve has an asymmetric relationship to the tumour (Fig. 9A) [16, 44], whereas the nerve passes through the centre of a neurofibroma or is obliterated by it. Cystic necrosis within schwannoma, so called ancient change, is a well-recognized variation [19, 45]. Tumours associated with cystic change do not exhibit the "target sign" and may be impossible to differentiate from MPNST (Fig. 9B) [19]. Neurofibromas and schwannomas are not associated with peritumoral oedema [20]. Mild muscle atrophy surrounding or distal to the tumour is also a recognized finding [15]. Intraspinal extension and the relationship to the cervical cord are best assessed on axial (Fig. 7) and coronal images (Fig. 10).

Malignant peripheral nerve sheath tumour (MPNST)

MPNSTs show no specific imaging features and may not be distinguishable from other soft-tissues sarcomas [18]. Therefore, great importance must be given to clinical features such as pain or rapid enlargement in the case of NF1. Features that help to differentiate benign and malignant neurogenic tumours include absence of the target sign on T2-weighted sequences [17, 19, 21], poorly defined margins (Figs. 11, 12) and bone destruction [16]. Inhomogeneous enhancement following gadolinium results from high intercellular pressure or areas of necrosis, another feature suggestive of malignancy (Fig. 13). However, as mentioned previously, inhomogeneous SI and absence of the "target sign" may occur with ancient schwannomas. The size of the lesion may also be unhelpful since many neurofibromas and some schwannomas may be multiple. The use of dynamic contrast-enhanced MRI has been reported to have a high diagnostic accuracy for differentiating benign and malignant soft-tissue masses. A large study by van der Woude et al. [46] assessed three enhancement characteristics and included seven schwannomas and a single MPNST. Three of seven schwannomas demonstrated early enhancement, a feature more commonly seen with malignant lesions. However, early peripheral enhancement and a type 1 pattern of progression of enhancement were highly specific for malignant lesions. Limited experience of diffusion-

Fig. 9 **A** Coronal T1-weighted SE image showing an oval lesion arising from the infraclavicular part of the left brachial plexus. The lesion has an asymmetrical relationship to the nerve of origin, indicating that it is a schwannoma. **B** Coronal T2-weighted FSE MR image showing the lesion to be inhomogeneous without the typical "target sign", consistent with ancient change

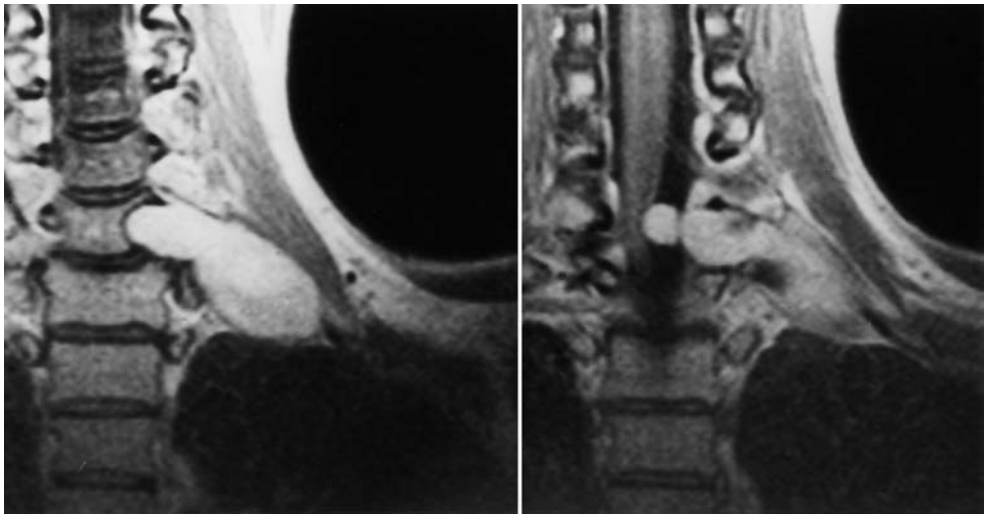

Fig. 10 Coronal post-contrast T1-weighted SE images in a patient with NF1 and a neurofibroma arising from the left C8 root. Well-defined erosion of the C7 vertebral body and intra-dural extension with cord compression are clearly demonstrated

weighted MRI of soft-tissue tumours suggests that differentiation between areas of viable tumour and necrosis is possible [47]. However, this technique has not been specifically applied to the assessment of neurogenic tumours.

Uptake of gallium citrate has been shown to be a feature of MPNST [14]. More recently, [^{18}F]fluorodeoxyglucose positron emission tomography (^{18}FDG PET) has been used with some success in identifying malignant change in plexiform neurofibromas [48]. However, whenever there is concern about malignant change, biopsy is recommended [14].

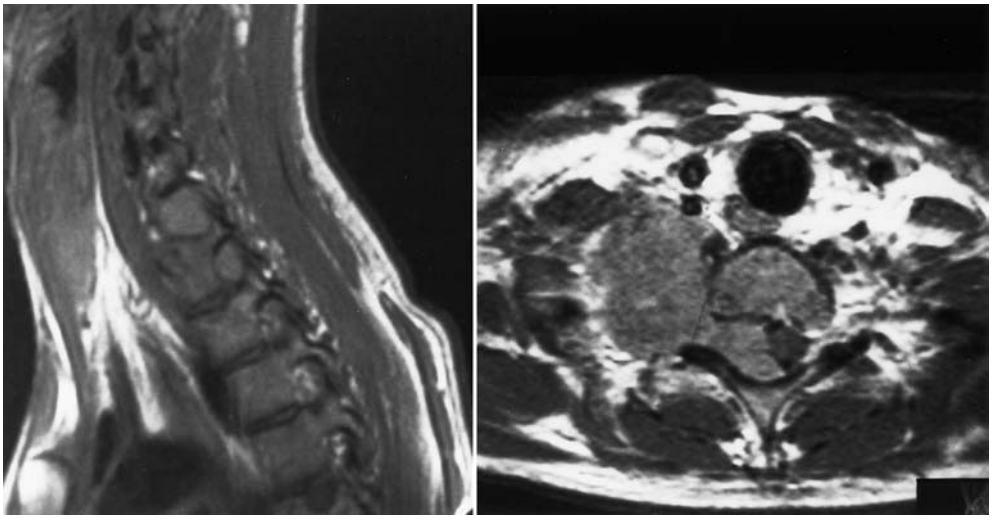

Fig. 11 Sagittal (*left*) and axial (*right*) T1-weighted SE images in a patient with MPNST of the right brachial plexus. The tumour extends through the C5/6 and C6/7 intervertebral foramina and forms a poorly defined extraspinal mass

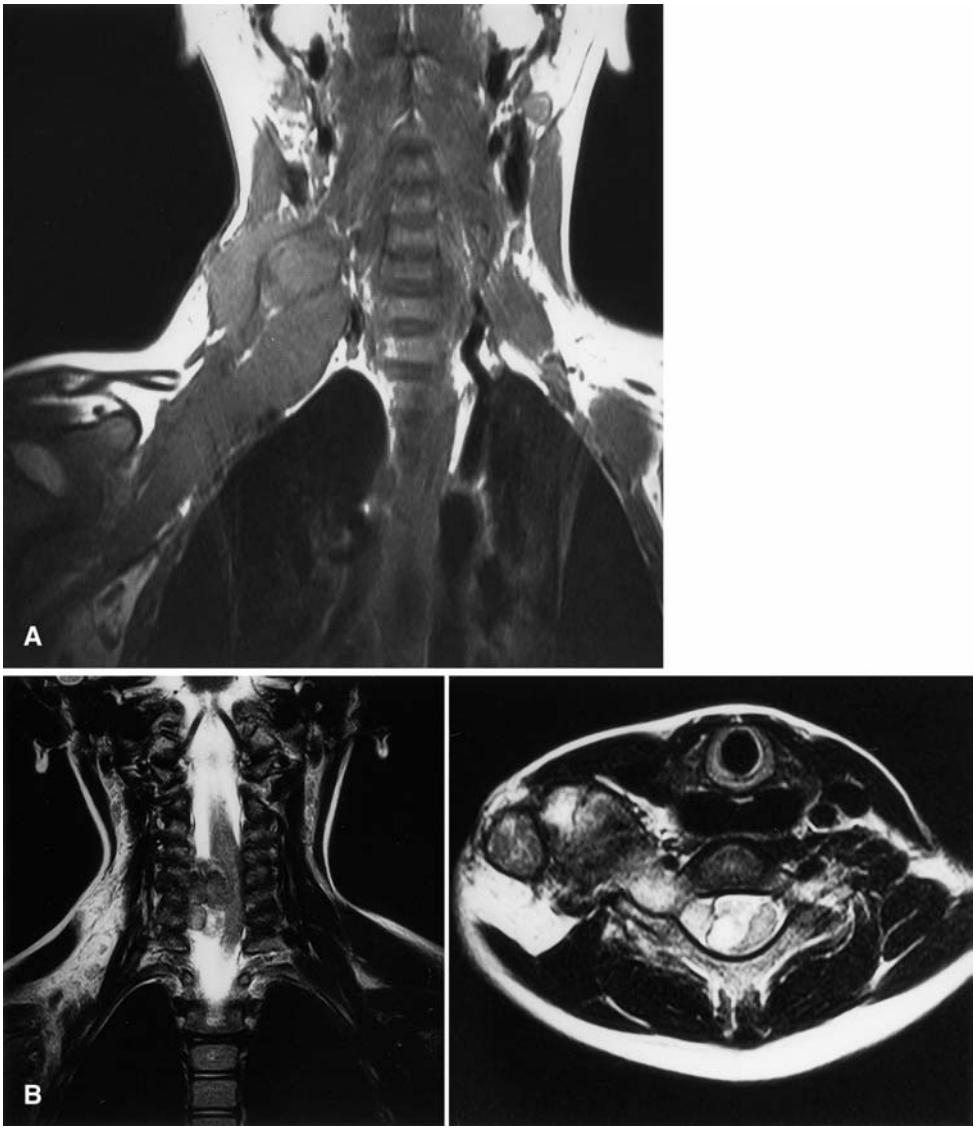

Fig. 12 **A** Coronal T1-weighted SE MR image in a young boy with MPNST arising from the right brachial plexus. The tumour is extensive and lobulated. **B** Coronal (*left*) and axial (*right*) T2-weighted FSE images showing the lesion to be inhomogeneous without a typical "target sign". Intradural extension and involvement of the right vertebral artery are also noted

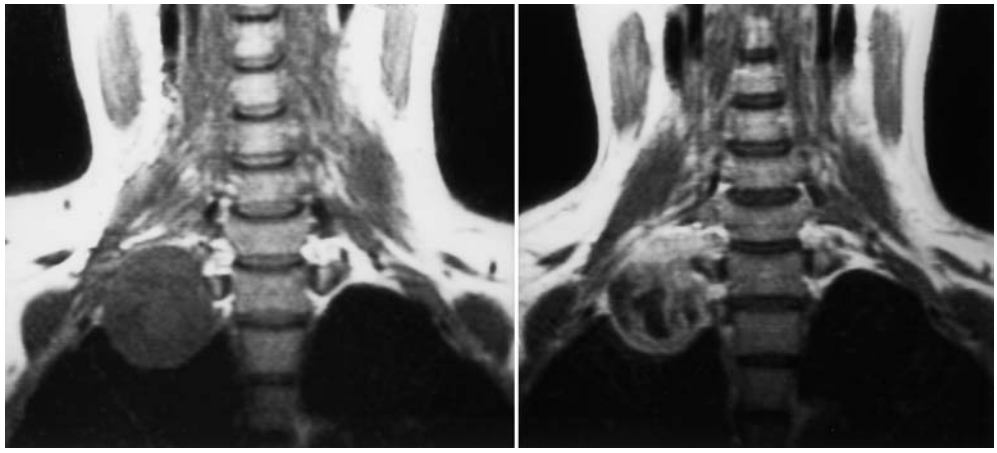

Fig. 13 Coronal T1-weighted SE images before (*left*) and after (*right*) intravenous contrast enhancement in a patient with MPNST arising from the lower roots of the right brachial plexus. Extensive areas of non-enhancement are present

Benign non-neurogenic tumours

The commonest benign non-neurogenic tumour to involve the brachial plexus is aggressive fibromatosis (extra-abdominal desmoid tumour). The tumour presents either as a painless mass or may be associated with pain or neurological dysfunction in the arm [49]. MRI typically shows a mass with infiltrative margins, which is isointense to muscle on T1-weighted sequences, hyperintense but inhomogeneous on T2-weighted sequences (Fig. 14) and which shows marked enhancement following intravenous contrast administration. Areas of signal void on T2-weighted images are also a characteristic feature, being due to regions of collagenous tissue within the mass [50, 51, 52]. Tumour margins may only be infiltrative at a microscopic level, in which case the lesion may appear well defined on MRI. The locally aggressive nature of the lesion makes identification of surgical margins difficult and local recurrence is a relatively common problem [53].

Lipoma is the second commonest benign non-neurogenic tumour to involve the brachial plexus and is well characterized by both CT and MRI due to its fatty nature (Fig. 15). However, the differentiation between lipoma and well-differentiated liposarcoma may be impossible on CT or MRI [54].

Various non-neoplastic lesions have also been described in relation to the brachial plexus. Localized hypertrophic neuropathy (perineurinoma, giant nerve) is a rare tumour-like lesion that typically involves a single peripheral nerve and produces slowly progressive weakness in the distribution of the nerve [55]. Involvement of the brachial plexus has been reported [56, 57]. MRI has demonstrated fusiform thickening of the affected nerve, which appears mildly hyperintense on T2-weighted images and shows enhancement following contrast administration [56]. However, the SI on T2-weighted images may also be diffusely reduced, differentiating the lesion from a nerve sheath tumour (Fig. 16). Other reported

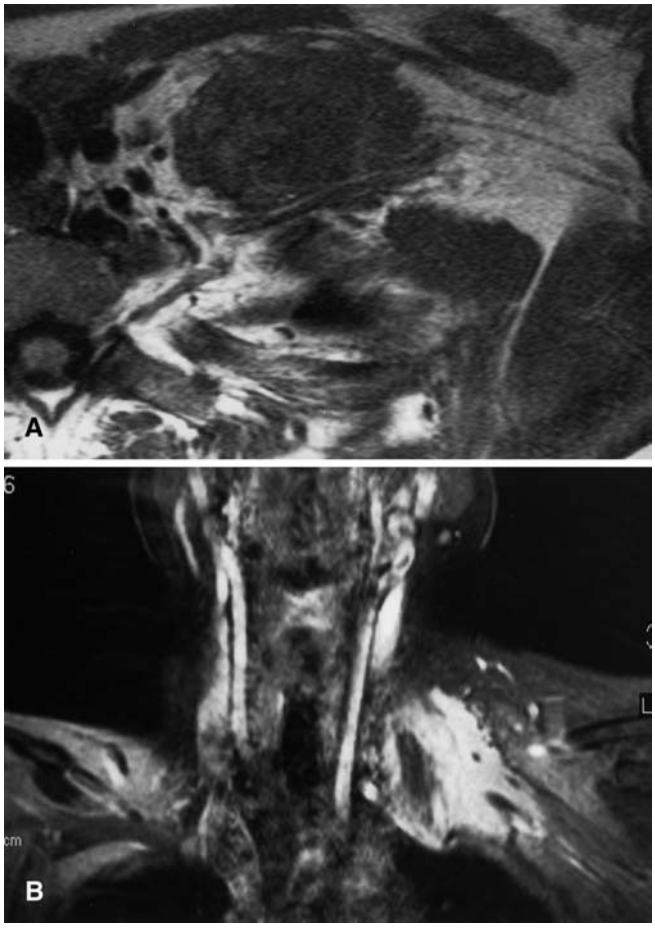

Fig. 14 **A** Axial T1-weighted SE image in a patient with aggressive fibromatosis involving the supraclavicular part of the left brachial plexus. The mass is isointense to muscle and has poorly defined, infiltrative margins. **B** Coronal STIR sequence shows the mass to be hyperintense. Note again the infiltrative nature of the margins

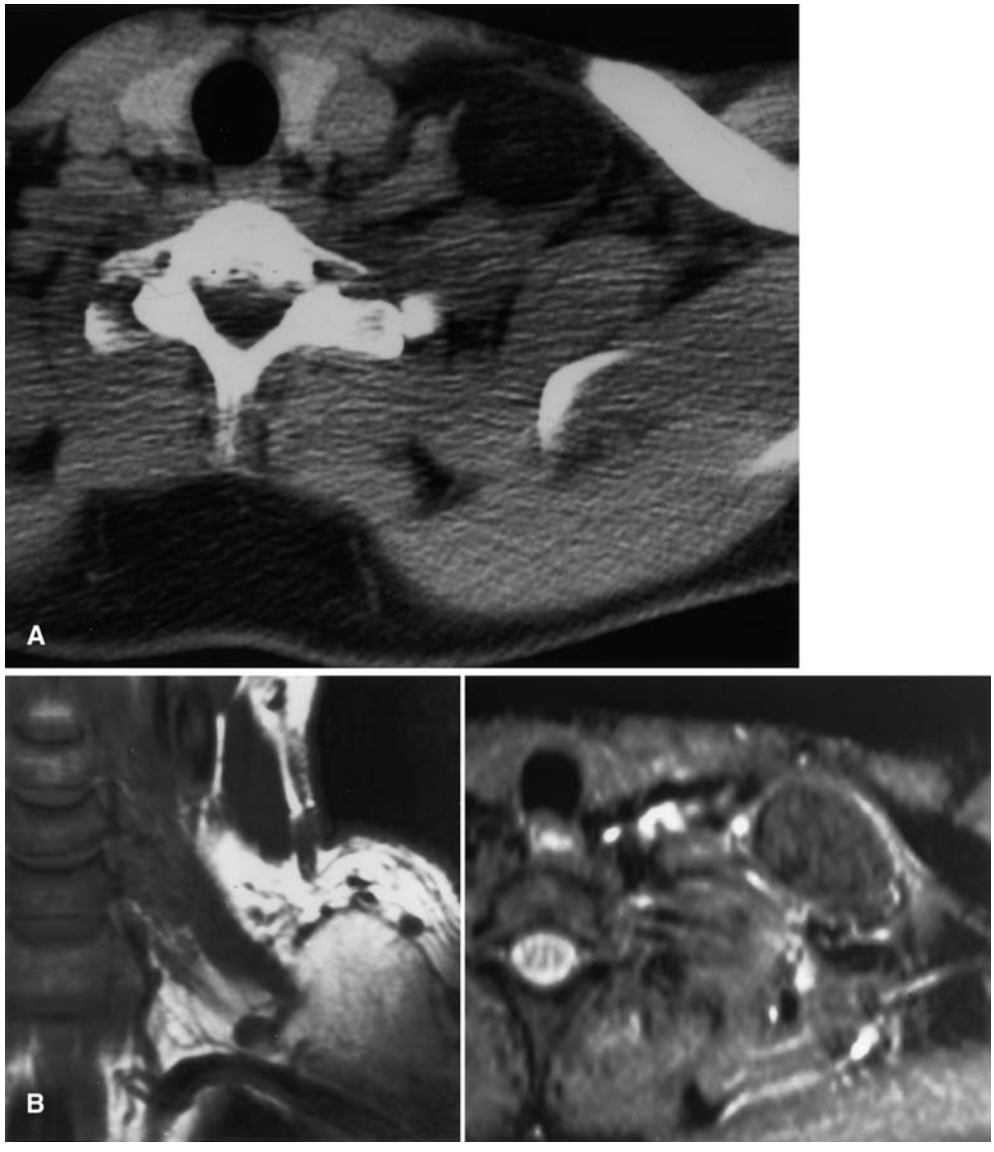

Fig. 15 Lipoma of the left brachial plexus. **A** Axial CT scan showing a well-defined, oval, hypodense mass in the left supraclavicular region. **B** Lipoma of the left brachial plexus. Coronal T1-weighted SE (*left*) and axial STIR (*right*) MR images showing a well-defined fatty mass in the left supraclavicular fossa

causes of diffuse swelling of the brachial plexus simulating tumour include chronic demyelinating hypertrophic neuropathy [57] and hypertrophic inflammatory neuropathy [58].

Fibrolipomatous hamartoma is a rare benign infiltrating condition of peripheral nerves leading to progressive functional loss, the lesion typically being located in the distal part of the upper limb, with the median nerve the commonest reported site. A single case has been reported in the brachial plexus [35]. MRI classically demonstrates fusiform nerve enlargement caused by fatty proliferation and thickening of nerve bundles [59].

Malignant non-neurogenic tumours

Malignant non-neurogenic tumours involving the brachial plexus include primary soft-tissue sarcomas (Figs. 5, 17), such as low-grade fibrosarcoma [53], synovial sarcoma [39] and radiation-induced sarcoma [36, 37, 38]. These tumours have no particular differentiating imaging features, although their malignant nature may be suggested by their dynamic enhancement patterns [46] and also by their clinical course, which includes pain and progressive neurological deficit. Radiation-induced sarcomas may develop as late as 40 years after radiotherapy [36], usually as a consequence of treatment for breast carcinoma. Radiotherapy has also been implicated in the development of approximately 11% of MPNSTs [60] (Fig. 18).

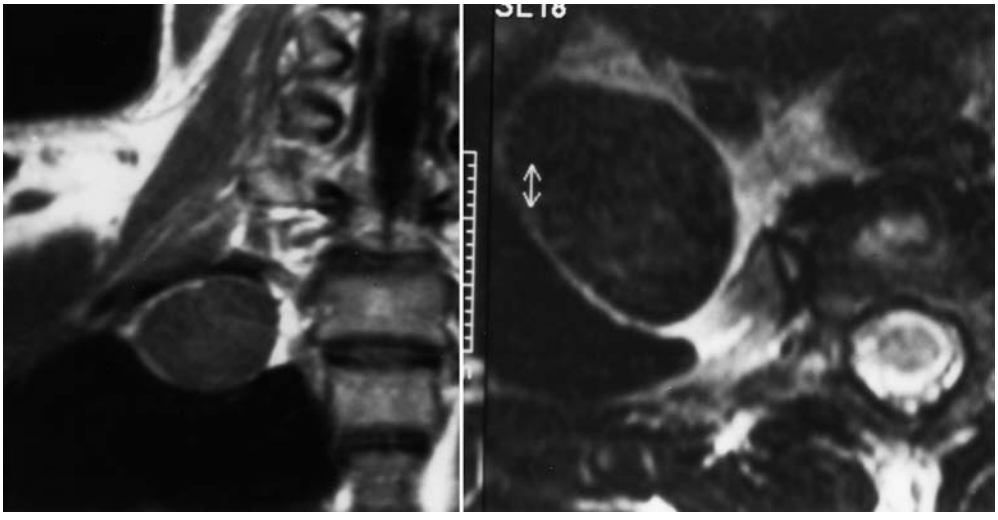

Fig. 16 Localized hypertrophic neuropathy. Coronal T1-weighted SE (*left*) and axial T2-weighted FSE (*right*) images showing a well-defined, oval lesion arising from the T1 root of the right brachial plexus. The lesion is isointense to muscle on T1 but profoundly hypointense on T2, differentiating it from a benign nerve sheath tumour

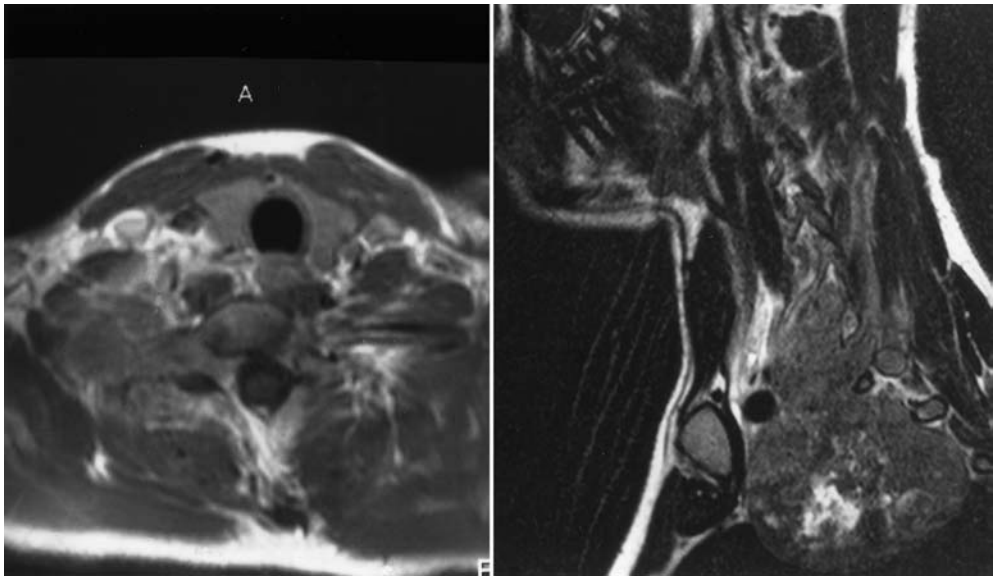

Fig. 17 Axial T1-weighted SE (*left*) and sagittal T2-weighted FSE (*right*) images of a young boy with primary soft-tissue Ewing sarcoma involving the right brachial plexus. The tumour has obliterated the subclavian artery

Fig. 18 Radiation-induced MPNST in a patient with NF1 who received radiotherapy 12 years previously for breast carcinoma. Coronal T1-weighted SE (*left*) and axial T2-weighted FSE (*right*) images show a large mass in the right axilla. Note the absence of the target sign

True haematogenous metastases to the plexus are rare. Meller et al. [61] reported five cases of proven metastasis to the plexus in which imaging studies including US, CT and MRI failed to demonstrate any mass lesion. The primary sites were the breast in three cases, the larynx in one case and a case of Hodgkin's lymphoma. Neurolymphoma is a rare manifestation of lymphoma in which peripheral nerve involvement is a dominant feature. It may occur in isolation or in association with systemic or primary central nervous system lymphoma. A single case of B-cell lymphoma with bilateral brachial plexus involvement has been reported where MRI showed diffuse swelling and hyperintensity on T2-weighted images with enhancement following gadolinium [40].

Conclusions

Tumours of the brachial plexus are uncommon. MRI has a major role in characterizing and staging such lesions. Benign neurogenic tumours can be confidently diagnosed if the classical imaging features are present together with a matching clinical picture. However, the presence of pain and neurological deficit indicates an aggressive process and MRI is unlikely to show diagnostic features. In such cases, pre-operative core needle biopsy is recommended.

References

1. Lusk MD, Kline DG, Garcia CA. Tumors of the brachial plexus. Neurosurgery 1987; 21:439–453.
2. Sheppard DG, Iyer RB, Fenstermacher MJ. Brachial plexus: demonstration at US. Radiology 1998; 208:402–406.
3. Retzl G, Kapral S, Greher M, Mauritz W. Ultrasonographic findings of the axillary part of the brachial plexus. Anesth Analg 2001; 92:1271–1275.
4. King AD, Ahuja AT, King W, Metreweli C. Sonography of peripheral nerve tumors of the neck. AJR Am J Roentgenol 1997; 169:1695–1698.
5. Simonovsky V. Peripheral nerve schwannoma preoperatively diagnosed by sonography: report of three cases and discussion. Eur J Radiol 1997; 25:47–51.
6. Castagno AA, Shuman WP. MR imaging in clinically suspected brachial plexus tumor. AJR Am J Roentgenol 1987; 149:1219–1222.
7. Rapoport S, Blair DN, McCarthy SM, Desser TS, Hammers LW, Sostman HD. Brachial plexus: correlation of MR imaging with CT and pathologic findings. Radiology 1988; 167:161–165.
8. Posniak HV, Olson MC, Dudiak CM, Wisniewski R, O'Malley C. MR imaging of the brachial plexus. AJR Am J Roentgenol 1993; 161:373–379.
9. de Verdier HJ, Colletti PM, Terk MR. MRI of the brachial plexus: a review of 51 cases. Comput Med Imaging Graph 1993; 17:45–50.
10. Sherrier RH, Sostman HD. Magnetic resonance imaging of the brachial plexus. J Thorac Imaging 1993; 8:27–33.
11. Bilbey JH, Lamond RG, Mattrey RF. MR imaging of disorders of the brachial plexus. J Magn Reson Imaging 1994; 4:13–18.
12. Wittenberg KH, Adkins MC. MR Imaging of non-traumatic brachial plexopathies: frequency and spectrum of findings. Radiographics 2000; 20:1023–1032.
13. van Es HW. MRI of the brachial plexus. Eur Radiol 2001; 11:325–336.
14. Levine E, Huntrakoon M, Wetzel LH. Malignant nerve-sheath neoplasms in neurofibromatosis: distinction from benign tumors by using imaging techniques. AJR Am J Roentgenol 1987; 149:1059–1064.
15. Stull MA, Moser RP Jr, Kransdorf MJ, Bogumill GP, Nelson MC. Magnetic resonance appearance of peripheral nerve sheath tumors. Skeletal Radiol 1991; 20:9-14.
16. Cerofolini E, Landi A, DeSantis G, Maiorana A, Canossi G, Romagnoli R. MR of benign peripheral nerve sheath tumors. J Comput Assist Tomogr 1991; 15:593–597.
17. Suh JS, Abenoza P, Galloway HR, Everson LI, Griffiths HJ. Peripheral (extracranial) nerve tumors: correlation of MR imaging and histologic findings. Radiology 1992; 183:341–346.
18. Verstraete KL, Achten E, De Schepper A, et al. Nerve sheath tumors: evaluation with CT and MR imaging. J Belge Radiol 1992; 75:311–320.
19. Varma DG, Moulopoulos A, Sara AS et al. MR imaging of extracranial nerve sheath tumors. J Comput Assist Tomogr 1992; 16:448–453.
20. Soderlund V, Goranson H, Bauer HC. MR imaging of benign peripheral nerve sheath tumors. Acta Radiol 1994; 35:282–286.
21. Bhargava R, Parham DM, Lasater OE, Chari RS, Chen G, Fletcher BD. MR imaging differentiation of benign and malignant peripheral nerve sheath tumors: use of the target sign. Pediatr Radiol 1997; 27: 124–129.
22. Beggs I. Pictorial review: imaging of peripheral nerve tumours. Clin Radiol 1997; 52:8-17.
23. Lin J, Martel W. Cross-sectional imaging of peripheral nerve sheath tumors: characteristic signs on CT, MR imaging, and sonography. AJR Am J Roentgenol 2001; 176:75–82.
24. Greenfield GB, Arrington JA, Kudryk BT. MRI of soft tissue tumors. Skeletal Radiol 1993; 22:77–84.
25. De Schepper AM, De Beuckeleer L, Vandevenne J, Somville J. Magnetic resonance imaging of soft tissue tumors. Eur Radiol 2000; 10: 213–223.
26. Siegel MJ. Magnetic resonance imaging of musculoskeletal soft tissue masses. Radiol Clin North Am 2001; 39:701–720.
27. Mukherji S, Castillo M, Wagle AG. The brachial plexus. Semin US CT MRI 1996; 17:519–538.
28. Sakai F, Sone S, Kiyono K, et al. Magnetic resonance imaging of neurogenic tumors of the thoracic inlet: determination of the parent nerve. J Thorac Imaging 1996; 11:272–278.
29. Sell PJ, Semple JC. Primary nerve tumours of the brachial plexus. Br J Surg 1987; 74:73–74.
30. Ogose A, Hotta T, Morita T. Tumors of peripheral nerves: correlation of symptoms, clinical signs, imaging features, and histologic diagnosis. Skeletal Radiol 1999; 28:183–188.

31. Boutsen Y, De Coene B, Hanson P, Deltombe T, Gilliard C, Esselinckx W. Axillary schwannoma masquerading as cervical radiculopathy. Clin Rheumatol 1999; 18:174–176.
32. Ganju A, Roosen N, Kline DG, Tiel RL. Outcomes in a consecutive series of 111 surgically treated plexal tumors: a review of the experience at the Louisiana State University Health Sciences Center. J Neurosurg 2001; 95:51–60.
33. Nakamichi K, Tachibana S. Intraneural ganglion of the branchial plexus. J Hand Surg [Br] 1998; 23:123-125.
34. Pechman D, Kenan S, Abdelwahab IF, Klein MJ, Lewis MM. Case report 839: Elastofibroma of the right shoulder causing brachial plexus impingement. Skeletal Radiol 1994; 23:459–461.
35. Price AJ, Compson JP, Calonje E. Fibrolipomatous hamartoma of nerve arising in the brachial plexus. J Hand Surg [Br] 1995; 20:16–18.
36. Foley KM, Woodruff JM, Ellis FT, Posner JB. Radiation-induced malignant and atypical peripheral nerve sheath tumors. Ann Neurol 1980; 7:311–318.
37. Gorson KC, Musaphir S, Lathi ES, Wolfe G. Radiation-induced malignant fibrous histiocytoma of the brachial plexus. J Neurooncol 1995; 26:73–77.
38. Hussussian CJ, Mackinnon SE. Postradiation neural sheath sarcoma of the brachial plexus: a case report. Ann Plast Surg 1999; 43:313–317.
39. Tacconi L, Thom M, Thomas DG. Primary monophasic synovial sarcoma of the brachial plexus: report of a case and review of the literature. Clin Neurol Neurosurg 1996; 98:249–252.
40. Swarnkar A, Fukui MB, Fink DJ, Rao GR. MR imaging of brachial plexopathy in neurolymphomatosis. AJR Am J Roentgenol 1997; 169:1189–1190.
41. Jeffery AR, Ellis FJ, Repka MX, Buncic JR. Pediatric Horner syndrome. J AAPOS 1998; 2:159–167.
42. Horowitz J, Kline DG, Keller SM. Schwannoma of the brachial plexus mimicking an apical lung tumor. Ann Thorac Surg 1991; 52:555–556.
43. Beggs I. The ring sign: a new ultrasound sign of peripheral nerve tumours. Clin Radiol 1998; 53:849–850.
44. Maiuri F, Donzelli R, Benvenuti D, Sardo L, Cirillo S. Schwannomas of the brachial plexus: diagnostic and surgical problems. Zentralbl Neurochir 2001; 62:93–97.
45. Romner B, Nygaard O, Ingebrigtsen T, Anke IM, Trumpy JH. Large peripheral cystic schwannomas. Two case reports and a review. Scand J Plast Reconstr Surg Hand Surg 1994; 28:231–234.
46. van der Woude HJ, Verstraete KL, Hogendoorn PCW, Taminiau AHM, Hermans J, Bloem JL. Musculoskeletal tumours: does fast dynamic contrast-enhanced subtraction MR imaging contribute to the characterization? Radiology 1998; 208:821–828.
47. Baur A, Reiser MF. Diffusion-weighted imaging of the musculoskeletal system in humans. Skeletal Radiol 2000; 29:555–562.
48. Ferner RE, Lucas JD, O'Doherty MJ, et al. Evaluation of [18]fluorodeoxyglucose positron emission tomography ([18]FDG PET) in the detection of malignant peripheral nerve sheath tumours arising from within plexiform neurofibromas in neurofibromatosis J Neurol Neurosurg Psychiatry 2000; 68:353–357.
49. Hoos A, Lewis JJ, Urist MJ, et al. Desmoid tumors of the head and neck: a clinical study of a rare entity. Head Neck 2000; 22:814–821.
50. O'Keefe F, Kim EE, Wallace S. Magnetic resonance imaging in aggressive fibromatosis. Clin Radiol 1990; 42:170–173.
51. Garant M, Remy H, Just N. Aggressive fibromatosis of the neck: MR findings. AJNR Am J Neuroradiol 1997; 18:1429–1431.
52. Robbin MR, Murphey MD, Temple HT, Kransdorf MJ, Choi JJ. Imaging of musculoskeletal fibromatosis. Radiographics 2001; 21:585–600.
53. Gaposchkin CG, Bilsky MH, Ginsberg R, Brennan MF. Function-sparing surgery for desmoid tumors and other low-grade fibrosarcomas involving the brachial plexus. Neurosurgery 1998; 42:1297–1301.
54. Kransdorf MJ, Bancroft LW, Peterson JJ, Murphey MD, Foster WC, Temple HT. Imaging of fatty tumors: distinction of lipoma and well-differentiated liposarcoma. Radiology 2002; 224:99–104.
55. Simmons Z, Mahadeen ZI, Kothari MJ, Powers S, Wise S, Towfighi J. Localized hypertrophic neuropathy: magnetic resonance imaging findings and long-term follow-up. Muscle Nerve 1999; 22:28–36.
56. Snyder M, Cancilla PA, Batzdorf U. Hypertrophic neuropathy simulating a neoplasm of the brachial plexus. Surg Neurol 1977; 7:131–134.
57. Van den Bergh PY, Thonnard JL, Duprez T, Laterre EC. Chronic demyelinating hypertrophic brachial plexus neuropathy. Muscle Nerve 2000; 23:283–288.
58. Stumpo M, Foschini MP, Poppi M, Cenacchi G, Martinelli P. Hypertrophic inflammatory neuropathy involving bilateral brachial plexus. Surg Neurol 1999; 52:458–464.
59. De Maeseneer M, Jaovisidha S, Lenchik L, et al. Fibrolipomatous hamartoma: MR imaging findings. Skeletal Radiol 1997; 26:155–160.
60. Ducatman BS, Scheithauer BW, Piepgras DG, Reiman HM, Ilstrup DM. Malignant peripheral nerve sheath tumors. A clinicopathologic study of 120 cases. Cancer 1986; 57:2006–2021.
61. Meller I, Alkalay D, Mozes M, Geffen DB, Ferit T. Isolated metastases to peripheral nerves. Report of five cases involving the brachial plexus. Cancer 1995; 76:1829–1832.